This article was downloaded by:
On: *23 January 2011*
Access details: *Access Details: Free Access*
Publisher *Taylor & Francis*
Informa Ltd Registered in England and Wales Registered Number: 1072954 Registered office: Mortimer House, 37-41 Mortimer Street, London W1T 3JH, UK

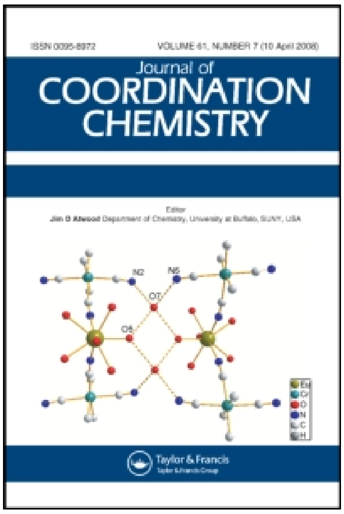

Journal of Coordination Chemistry

Publication details, including instructions for authors and subscription information:
http://www.informaworld.com/smpp/title~content=t713455674

Ternary copper(II) malonato complexes with alkali metals: $K_2Cu(mal)_2 \cdot 3H_2O$, $Rb_2Cu(mal)_2 \cdot H_2O$, $Cs_2[Cu(H_2O)_2(mal)_2]\ 2H_2O$

Yue-Qing Zheng[a]; Er-Bo Ying[a]
[a] Municipal Key Laboratory of Solid Materials Chemistry, Institute of Inorganic Chemistry, Ningbo 315211, P.R. China

To cite this Article Zheng, Yue-Qing and Ying, Er-Bo(2006) 'Ternary copper(II) malonato complexes with alkali metals: $K_2Cu(mal)_2 \cdot 3H_2O$, $Rb_2Cu(mal)_2 \cdot H_2O$, $Cs_2[Cu(H_2O)_2(mal)_2]\ 2H_2O$', Journal of Coordination Chemistry, 59: 11, 1281 — 1293

To link to this Article: DOI: 10.1080/00958970500491044

URL: http://dx.doi.org/10.1080/00958970500491044

PLEASE SCROLL DOWN FOR ARTICLE

Full terms and conditions of use: http://www.informaworld.com/terms-and-conditions-of-access.pdf

This article may be used for research, teaching and private study purposes. Any substantial or systematic reproduction, re-distribution, re-selling, loan or sub-licensing, systematic supply or distribution in any form to anyone is expressly forbidden.

The publisher does not give any warranty express or implied or make any representation that the contents will be complete or accurate or up to date. The accuracy of any instructions, formulae and drug doses should be independently verified with primary sources. The publisher shall not be liable for any loss, actions, claims, proceedings, demand or costs or damages whatsoever or howsoever caused arising directly or indirectly in connection with or arising out of the use of this material.

Journal of Coordination Chemistry
Vol. 59, No. 11, 20 July 2006, 1281–1293

Taylor & Francis
Taylor & Francis Group

Ternary copper(II) malonato complexes with alkali metals: $K_2Cu(mal)_2 \cdot 3H_2O$, $Rb_2Cu(mal)_2 \cdot H_2O$, $Cs_2[Cu(H_2O)_2(mal)_2]\ 2H_2O$

YUE-QING ZHENG* and ER-BO YING

Municipal Key Laboratory of Solid Materials Chemistry,
Institute of Inorganic Chemistry, Ningbo 315211, P.R. China

(*Received in final form 13 July 2005*)

Reactions of copper(II) chloride and malonic acid with the corresponding alkali metal carbonate in the presence of imidazole in aqueous methanol at $pH = 4.2–6.0$ yielded $K_2Cu(mal)_2 \cdot 3H_2O$ (**1**), $Rb_2Cu(mal)_2 \cdot H_2O$ (**2**) and $Cs_2[Cu(H_2O)_2(mal)_2] \cdot 2H_2O$ (**3**) (H_2mal = malonic acid). In **1**, octahedrally coordinated Cu atoms are interlinked by malonate anions to generate 2D ${}^{2}_{\infty}[Cu(mal)_{4/2}]^{2-}$ anionic layers, between which the K^+ cations are sandwiched. The 1D anionic ${}^{1}_{\infty}[Cu(mal)(mal)_{2/2}]^{2-}$ chain in **2** is generated from square pyramidally coordinated Cu atoms bridged by malonate anions and is held together by Rb^+ cations. The cesium compound consists of Cs^+ cations and *trans*-$[Cu(H_2O)_2(mal)_2]^{2-}$ anions with Cu atoms octahedrally coordinated. Diminution in dimensionality from the 2D ${}^{2}_{\infty}[Cu(mal)_{4/2}]^{2-}$ anionic layer in **1** through the 1D anionic ${}^{1}_{\infty}[Cu(mal)(mal)_{2/2}]^{2-}$ chain in **2** to *trans*-$[Cu(H_2O)_2(mal)_2]^{2-}$ anions in **3** could be attributed to the replacement of the smaller alkali cation by the larger one. IR spectroscopic, magnetic and thermal data are discussed.

Keywords: Copper; Alkali metal; Malonate; Coordination polymer; Crystal structure; Properties

1. Introduction

The past decade has witnessed rapidly growing interest in the utilization of benezene carboxylic di-, tri- and polycarboxylic acids to rational design and synthesis of hybrid inorganic–organic materials [1–3]. In contrast to these rigid bridging ligands, aliphatic α,ω-dicarboxylate anions are flexible ligands due to their conformational and coordination variability [4–7]. Therefore, construction of coordination polymers based on α,ω-dicarboxylate anions is of current interest and it is expected that the flexibility of such dicarboxylato ligands might prevent collapse of the structure upon removal of guest molecules. As a lower member of the α,ω-dicarboxylate family, the malonate ligand, with two neighboring carboxylate groups, is a very flexible ligand which can adopt a monodentate binding mode, various bischelating modes and

---

*Corresponding author. Email: zhengcm@nbu.edu.cn

Journal of Coordination Chemistry
ISSN 0095-8972 print: ISSN 1029-0389 online
DOI: 10.1080/00958970500491044

different carboxylate bridging modes (*syn*-*syn*, *syn*-*anti*, and *anti*-*anti*) [8], and research has been driven by interest in establishing magneto-structure correlation of malonato complexes [9]. In recent years, we have focussed on the construction of coordination polymers based on α,ω-dicarboxylato ligands [10, 11] and we report here the syntheses and characterization of three ternary copper(II) malonato complexes with alkali metals, $K_2Cu(mal)_2 \cdot 3H_2O$ (**1**), $Rb_2Cu(mal)_2 \cdot H_2O$ (**2**) and $Cs_2[Cu(H_2O)_2(mal)_2] \cdot 2H_2O$ (**3**) (H_2mal = malonic acid); these were obtained by reactions of copper(II) chloride and malonic acid with the corresponding alkali metal carbonate in the presence of imidazole in aqueous methanol at pH = 4.2–6.0.

2. Experimental

2.1. *Physical measurements*

All chemicals of reagent grade were commercially available and used without further purification. Elemental analyses (carbon and hydrogen) were performed using a Perkin-Elmer 2400II CHNS/O instrument. IR spectra (KBr pellets) in the range 4000–400 cm^{-1} were recorded using a Shimadzu FTIR-8900 spectrophotometer. Combined thermogravimetric and differential thermal analyses (TG/DTA), using Seiko Exstar6000 TG/DTA6300 equipment, were carried out on powdered samples in a nitrogen stream over 25–600°C with a heating rate of 10°C min^{-1}. Magnetic measurements were performed on polycrystalline samples with a Quantum Design MPMS-7 SQUID magnetometer with an applied field of 10000 G in the temperature range 5–300 K. Diamagnetic corrections were estimated from Pascal's constants [12].

2.2. *Syntheses*

2.2.1. $K_2Cu(mal)_2 \cdot 3H_2O$ (1). Some 24.0 cm^3 of 0.2 M K_2CO_3 were added to an aqueous methanolic solution of 0.170 g (2.50 mmol) of imidazole, 0.260 g (2.50 mmol) of malonic acid and 0.426 g (2.50 mmol) of $CuCl_2 \cdot 2H_2O$ in 50 cm^3 of CH_3OH/H_2O (1 : 1 v/v) to give a dark blue solution (pH = 9.08), which was adjusted to pH = 5.95 by adding malonic acid. Slow evaporation at room temperature during several weeks afforded pale blue plate-like crystals. Yield: ca 20% based on initial $CuCl_2 \cdot 2H_2O$. Anal. Calcd for $C_6H_{10}CuK_2O_{11}$ (%): C, 18.00; H, 2.50. Found: C, 18.01; H, 2.50. IR (cm^{-1}): 3418s, 2924w, 1589vs, 1423vs, 1389s, 1356s, 1281m, 1178w, 978s, 937m, 822m, 743m, 563m, 571w.

2.2.2. $Rb_2Cu(mal)_2 \cdot H_2O$ (2). Some 10.0 cm^3 of 0.2 M Rb_2CO_3 were added to an aqueous methanolic solution of 0.170 g (2.50 mmol) of imidazole, 0.260 g (2.50 mmol) of malonic acid and 0.426 g (2.50 mmol) of $CuCl_2 \cdot 2H_2O$ in 50 cm^3 of CH_3OH/H_2O (1 : 1 v/v) to give a dark blue solution (pH = 9.07), which was adjusted to pH = 5.35 by adding malonic acid. Slow evaporation at room temperature during several weeks afforded blue plate-like crystals. Yield: ca 20% based on initial $CuCl_2 \cdot 2H_2O$. Anal. Calcd for $C_6H_6CuO_9Rb_2$ (%): C, 15.34; H, 1.29. Found: C, 15.34; H, 1.28.

IR (cm^{-1}): 3381m, 2903vw, 1582vs, 1427s, 1381m, 1360m, 1281w, 1190vw, 970m, 935w, 810w, 745m, 671vw, 623vw, 550vw, 446vw.

2.2.3. $Cs_2[Cu(H_2O)_2(mal)_2] \cdot 2H_2O$ (3). Some 10.0 cm^3 of 0.2 M Cs_2CO_3 were added to an aqueous methanolic solution of 0.170 g (2.50 mmol) of imidazole, 0.260 g (2.50 mmol) of malonic acid and 0.426 g (2.50 mmol) of $CuCl_2 \cdot 2H_2O$ in 50 cm^3 of CH_3OH/H_2O (1 : 1 v/v) to give a dark blue solution (pH = 9.43), which was adjusted to pH = 4.2 by adding malonic acid. Slow evaporation at room temperature over several weeks afforded pale blue crystals. Yield: ca 30% based on initial $CuCl_2 \cdot 2H_2O$. Anal. Calcd for $C_6H_{12}Cs_2CuO_{12}$ (%): C, 11.88; H, 1.98. Found: C, 11.86; H, 1.99. IR (cm^{-1}): 3441m, 3242w, 1670w, 1597vs, 1429s, 1387m, 1356m, 1273w, 1180w, 972w, 962w, 934w, 812w, 735m, 687vw, 671vw, 652vw, 575w, 444vw.

2.3. *X-ray crystallography*

A suitable single crystal of each compound was carefully selected under a polarizing microscope and glued at the tip of a thin glass fibre, which was then mounted on a Bruker P4 diffractometer with graphite-monochromated Mo Kα radiation ($\lambda = 0.71073$ Å) for cell determination and subsequent data collection. Lattice parameters were refined from the 2θ values (10–25°) of 25 carefully centred reflections. Reflection intensities with $2\theta_{max} = 55°$ were collected at 293 K using the θ–2θ scan technique. On the basis of monitored reflections, the crystals exhibited no detectable decay during data collection. Data were corrected for Lp and absorption effects. SHELXS-97 and SHELXL-97 programs [13, 14] were used for structure solution and refinement. The structures were solved by direct methods. Subsequent difference Fourier syntheses enabled all non-hydrogen atoms to be located. After several cycles of refinement, all hydrogen atoms of malonate anions were geometrically generated while the hydrogen atoms of water molecules were located from successive difference Fourier syntheses. Finally, all non-hydrogen atoms were refined with anisotropic displacement parameters by full-matrix least-squares techniques and hydrogen atoms with isotropic displacement parameters. Details concerning crystal data and structure determinations are summarized in table 1. Selected interatomic distances and bond angles are given in tables 2 to 4.

3. Results and discussion

3.1. *Syntheses and characterization*

The ternary compounds resulted from reaction of copper(II) chloride and malonic acid with the corresponding alkali metal carbonate in the presence of imidazole in aqueous methanol at pH = 4.2–6.0. The reactions were originally initiated to synthesize new Cu(II) imidazole malonato complexes for a systematic investigation on transition metal dicarboxylato complexes with heteroaromatic *N*-donor ligands [15, 16]. In the present cases, no Cu(II) imidazole malonato complexes were isolated. Repeated experiments

Table 1. Summary of crystal data, data collection, structure solution and refinement details for 1, 2 and 3.

Compound	**1**	**2**	**3**
Empirical formula	$C_6H_{10}CuK_2O_{11}$	$C_6H_6CuO_9Rb_2$	$C_6H_{12}Cs_2CuO_{12}$
Formula weight	399.89	456.59	605.52
Description	Blue block	Blue plate	Pale blue plate
Crystal size (mm^3)	0.42 × 0.31 × 0.18	0.46 × 0.42 × 0.09	0.40 × 0.24 × 0.09
Temperature (K)	293(2)	293(2)	293(2)
Crystal system	Orthorhombic	Orthorhombic	Triclinic
Space group	*Pbcn*	$P2_12_12_1$	$P\bar{1}$
Unit cell dimensions			
a (Å)	7.420(2)	7.220(1)	7.116(1)
b (Å)	18.844(4)	9.460(2)	7.128(1)
C (Å)	9.320(2)	17.024(3)	7.516(2)
α (°)			87.34(3)
β (°)			79.45(3)
γ (°)			86.68(3)
Volume (Å^3)	1303.1(5)	1162.8(4)	373.9(1)
Z	4	4	1
D_{Calcd} (g cm^{-3})	2.038	2.608	2.689
$F(000)$	804	868	283
μ (mm^{-1})	2.332	10.193	6.282
Absorption correction	Empirical; Psi-scan		
Refinement method	Full-matrix least-squares on F^2		
θ range (°)	2.16–27.49	2.39–27.50	2.76–27.49
Reflections collected	2048	2102	2132
Unique reflections (R_{int})	1504 (0.0315)	1930 (0.0758)	1716 (0.0148)
Data, restraints, parameters	1145, 0, 114	1711, 0, 165	1667, 0, 115
Goodness of fit on F^2	1.077	1.089	1.145
R_1, wR_2 $[I \geq 2\sigma(I)]^a$	0.0429, 0.1108	0.0775, 0.1849	0.0324, 0.0874
R_1, wR_2 (all data)^a	0.0558, 0.1221	0.0835, 0.1938	0.0330, 0.0883
Extinction coefficients	0.025(2)	0.010(2)	0.082(5)
A, B values in w^b	0.0663, 0.5948	0.1555, 0.0000	0.0588, 0.2058
$\Delta\rho_{\max}$, $\Delta\rho_{\min}$ (e Å^{-3})	0.716, –0.963	1.034, −2.251	1.187, –1.348

[a] $wR_2 = [\sum w(F_o^2 - F_c^2)^2 / \sum w(F_o^2)^2]^{1/2}$. [b] $w = [\sigma^2(F_o^2) + (AP)^2 + BP]^{-1}$ with $P = (F_o^2 + 2F_c^2)/3$.

Table 2. Selected interatomic distances (Å) and bond angles (°) for **1**.

Cu–O(1)	1.939(2)	K(1)–O(2)$^{\#4}$	2.687(2)	K(2)–O(1)$^{\#1}$	2.751(2)
Cu–O(1)$^{\#1}$	1.939(2)	K(1)–O(3)$^{\#5}$	2.831(2)	K(2)–O(2)$^{\#8}$	2.916(3)
Cu–O(3)	1.941(2)	K(1)–O(3)$^{\#6}$	2.831(2)	K(2)–O(2)$^{\#9}$	2.916(3)
Cu–O(3)$^{\#1}$	1.941(2)	K(1)–O(5)$^{\#7}$	2.783(3)	K(2)–O(5)	2.684(3)
Cu–O(4)$^{\#2}$	2.689(2)	K(1)–O(5)$^{\#8}$	2.783(3)	K(2)–O(5)$^{\#1}$	2.684(3)
Cu–O(4)$^{\#3}$	2.689(2)	K(1)–O(6)	2.784(5)		
K(1)–O(2)	2.687(2)	K(2)–O(1)	2.751(2)		
O(1)–Cu–O(1)$^{\#1}$	87.9(1)	O(1)$^{\#1}$–Cu–O(3)	173.25(8)	O(3)–Cu–O(4)$^{\#2}$	97.78(8)
O(1)–Cu–O(3)	92.55(8)	O(1)$^{\#1}$–Cu–O(3)$^{\#1}$	92.55(8)	O(3)–Cu–O(4)$^{\#3}$	89.77(7)
O(1)–Cu–O(3)$^{\#1}$	173.25(8)	O(1)$^{\#1}$–Cu–O(4)$^{\#2}$	88.97(8)	O(3)$^{\#1}$–Cu–O(4)$^{\#2}$	89.77(7)
O(1)–Cu–O(4)$^{\#2}$	83.50(8)	O(1)$^{\#1}$–Cu–O(4)$^{\#3}$	83.50(8)	O(3)$^{\#1}$–Cu–O(4)$^{\#3}$	97.78(8)
O(1)–Cu–O(4)$^{\#3}$	88.97(8)	O(3)–Cu–O(3)$^{\#1}$	87.8(1)	O(4)$^{\#2}$–Cu–O(4)$^{\#3}$	169.54(8)
Hydrogen bonding contacts					
D–H	d(D–H)	d(H ··· A)	∠(D–H ··· A)	d(D–H ··· A)	A
O(5)–H(5A)	0.78	2.15	141	2.796	O(2)$^{\#1}$
O(5)–H(5B)	0.76	2.03	165	2.764	O(4)$^{\#10}$
O(6)–H(6)	0.70	2.64	156	3.289	O(1)$^{\#11}$

Symmetry codes: 1 = –x + 1, y, –z + 1/2; #2 = –x + 1/2, –y + 1/2, z–1/2; #3 = x + 1/2, −y + 1/2, –z + 1; #4 = –x, y, –z + 3/2; #5 = –x + 1/2, –y + 1/2, z + 1/2; #6 = x–1/2, –y + 1/2, –z + 1; #7 = x–1, –y, z + 1/2; #8 = –x + 1, –y, –z + 1; #9 = x, –y, z–1/2; #10 = x + 1/2, y–1/2, –z + 1/2; #11 = –x, –y, –z + 1.

Table 3. Selected interatomic distances (Å) and bond angles (°) for **2**.

Cu–O(1)	1.923(8)	Rb(1)–O(4)$^{\#4}$	3.152(9)	Rb(2)–O(2)	3.070(9)
Cu–O(3)	1.917(8)	Rb(1)–O(5)	3.054(9)	Rb(2)–O(2)$^{\#3}$	2.84(1)
Cu–O(4)$^{\#1}$	2.597(1)	Rb(1)–O(6)	3.658(9)	Rb(2)–O(3)$^{\#7}$	3.493(8)
Cu–O(5)	1.930(8)	Rb(1)–O(6)$^{\#5}$	3.08(1)	Rb(2)–O(5)	3.599(8)
Cu–O(7)	1.918(8)	Rb(1)–O(8)$^{\#6}$	2.815(9)	Rb(2)–O(6)$^{\#8}$	2.751(9)
Rb(1)–O(1)$^{\#2}$	3.10(1)	Rb(1)–O(9)	2.97(1)	Rb(2)–O(7)$^{\#7}$	2.888(8)
Rb(1)–O(2)$^{\#3}$	3.107(9)	Rb(1)–O(9)$^{\#5}$	3.663(9)	Rb(2)–O(8)$^{\#7}$	3.26(1)
Rb(1)–O(2)$^{\#2}$	3.50(1)	Rb(2)–O(1)	2.977(8)	Rb(2)–O(9)	2.83(1)
O(1)–Cu–O(3)	92.1(3)	O(3)–Cu–O(4)$^{\#1}$	97.7(4)	O(4)$^{\#1}$–Cu–O(7)	91.1(3)
O(1)–Cu–O(4)$^{\#1}$	84.5(4)	O(3)–Cu–O(5)	167.3(4)	O(5)–Cu–O(7)	90.8(3)
O(1)–Cu–O(5)	89.3(4)	O(3)–Cu–O(7)	88.9(4)		
O(1)–Cu–O(7)	175.5(4)	O(4)$^{\#1}$–Cu–O(5)	95.0(4)		
Hydrogen bonding contacts					
D–H	d(D–H)	d(H···A)	∠(D–H···A)	d(D–H···A)	A
O(9)–H(9A)	0.77	2.02	170	2.782	O(6)
O(9)–H(9B)	0.83	2.06	159	2.853	O(4)$^{\#7}$
O(9)–H(9B)	0.83	2.47	138	3.131	O(3)$^{\#7}$

Symmetry codes: $1 = -x+2,\ y+1/2,\ -z+3/2$; $\#2 = x-1,\ y,\ z$; $\#3 = x-1/2,\ -y+1/2,\ -z+2$; $\#4 = -x+1,\ y+1/2,\ -z+3/2$; $\#5 = x-1/2,\ -y+3/2,\ -z+2$; $\#6 = -x+1,\ y-1/2,\ -z+3/2$; $\#7 = -x+3/2,\ -y+1,\ z+1/2$; $\#8 = x+1/2,\ -y+3/2,\ -z+2$.

Table 4. Selected interatomic distances (Å) and bond angles (°) for **3**.

Cu–O(1)	1.971(2)	Cs–O(1)$^{\#2}$	3.446(3)	Cs–O(4)$^{\#5}$	3.037(3)
Cu–O(1)$^{\#1}$	1.971(2)	Cs–O(2)	4.140(3)	Cs–O(5)	4.104(4)
Cu–O(3)	1.936(3)	Cs–O(2)$^{\#3}$	3.116(3)	Cs–O(5)$^{\#6}$	3.716(4)
Cu–O(3)$^{\#1}$	1.936(3)	Cs–O(2)$^{\#4}$	3.862(4)	Cs–O(6)	3.298(5)
Cu–O(5)	2.418(3)	Cs–O(2)$^{\#2}$	3.403(4)	Cs–O(6)$^{\#4}$	3.392(4)
Cu–O(5)$^{\#1}$	2.418(3)	Cs–O(3)$^{\#1}$	3.038(3)		
Cs–O(1)	3.210(3)	Cs–O(4)$^{\#1}$	3.811(3)		
O(1)–Cu–O(1)$^{\#1}$	180.0(1)	O(1)$^{\#1}$–Cu–O(3)	87.0(1)	O(3)–Cu–O(5)	92.6(1)
O(1)–Cu–O(3)	93.0(1)	O(1)$^{\#1}$–Cu–O(3)$^{\#1}$	93.0(1)	O(3)–Cu–O(5)$^{\#1}$	87.4(1)
O(1)–Cu–O(3)$^{\#1}$	87.0(1)	O(1)$^{\#1}$–Cu–O(5)	85.2(1)	O(3)$^{\#1}$–Cu–O(5)	87.4(1)
O(1)–Cu–O(5)	94.8(1)	O(1)$^{\#1}$–Cu–O(5)$^{\#1}$	94.8(1)	O(3)$^{\#1}$–Cu–O(5)$^{\#1}$	92.6(1)
O(1)–Cu–O(5)$^{\#1}$	85.2(1)	O(3)–Cu–O(3)$^{\#1}$	180.00	O(5)–Cu–O(5)$^{\#1}$	180.0(2)
Hydrogen bonding contacts					
D–H	d(D–H)	d(H···A)	∠(D–H···A)	d(D–H···A)	A
O(5)–H(5A)	0.77	2.06	154	2.773	O(6)$^{\#4}$
O(5)–H(5B)	0.72	2.02	160	2.704	O(4)$^{\#3}$
O(6)–H(6A)	0.73	2.20	141	2.814	O(5)$^{\#6}$
O(6)–H(6B)	0.57	2.20	161	2.746	O(2)

Symmetry codes: $1 = -x,\ -y,\ -z+1$; $\#2 = -x,\ -y,\ -z$; $\#3 = x,\ y+1,\ z$; $\#4 = -x+1,\ -y,\ -z$; $\#5 = x,\ y+1,\ z-1$; $\#6 = x,\ y,\ z-1$.

indicated that an appropriate amount of imidazole is essential for the growth of crystals suitable for X-ray analysis.

The infrared spectrum of **1** showed an asymmetric OCO stretch (ν_{as}(OCO)) at 1589 cm^{-1}, symmetric OCO stretching vibrations (ν_s(OCO)) at 1423, 1389 and 1356 cm^{-1}, and OCO bending (ν(OCO)) at 822 and 743 cm^{-1} [17]. Strong ν_{as}(OCO) absorptions appear at 1582 cm^{-1} and 1597 cm^{-1} for **2** and **3**, respectively. Absorptions at 1427, 1381 and 1360 cm^{-1} for **2** and at 1429, 1387 and 1356 cm^{-1} for **3** could be assigned to the symmetric OCO stretching. The ν(OCO) bending absorptions were observed at 810 and 745 cm^{-1} for **2** and at 812 and 735 cm^{-1} for **3**. Broad bands of medium to strong intensity centred at 3418, 3381 and 3441 cm^{-1} for **1**, **2** and **3**, respectively, confirm the presence of water molecules.

Table 5. Thermal decomposition data for **1**, **2** and **3**.

Compound	T(°C)	Weight loss (%) obs.	Weight loss (%) theor.	Lost in reaction
1	27–127	13.6	13.52	3 H_2O
	237–278	24.0	23.52	0.5 $C_2H_4 + (C_3H_2O_3)$
	341–453	7.0	7.0	CO
2	42–180	3.5	3.94	H_2O
	230–279	20.0	20.59	0.5 $C_2H_4 + (C_3H_2O_3)$
	330–460	6.0	6.13	CO
3	20–90	11.80	11.90	4 H_2O
	220–280	15.5	15.53	0.5 $C_2H_4 + (C_3H_2O_3)$
	372–465	4.6	4.63	CO

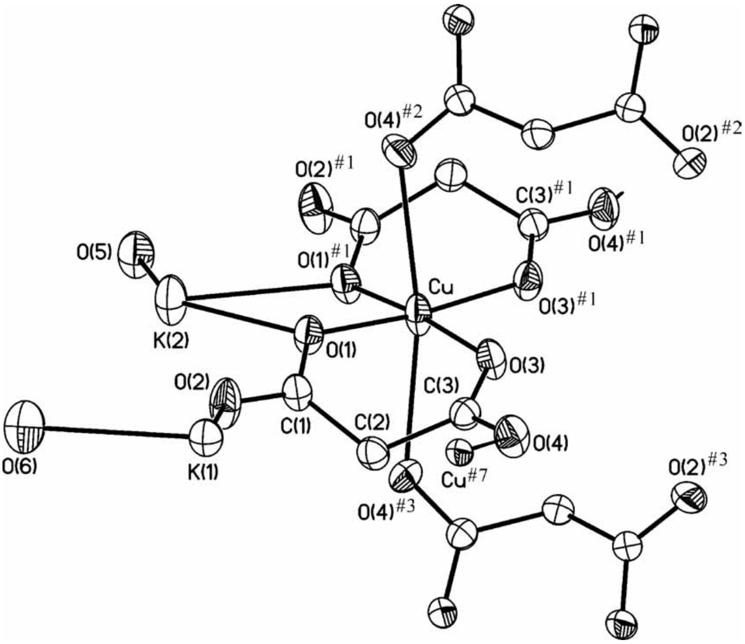

Figure 1. Ortep view of the coordination environment around Cu with the atom labelling for **1** (displacement ellipsoids drawn at 45% probability).

Magnetic measurements over the temperature range 5–300 K indicated that the complexes obey the Curie–Weiss law $\chi_m(T–\theta) = C$ with the Curie constants of 0.417(2), 0.423(2) and 0.411(3) $cm^3\,K\,mol^{-1}$ for **1**, **2** and **3**, respectively, as well as the corresponding Weiss constant $\theta = 4.2(6)$, 3.0(6), 4.3(9) K, indicative of overall weak ferromagnetic coupling between Cu^{2+} centres. Effective magnetic moments at room temperature are 1.81, 1.82 and 1.78μ_B for **1**, **2** and **3**, respectively, practically identical to the spin-only value of 1.73μ_B of the free Cu^{2+} ion [12].

The combined TG–DTA curves showed that the complexes decompose in three steps (table 5); from room temperature to ca 80°C, endothermic dehydration gives anhydrous malonates $A_2Cu(mal)_2$ with A = K, Rb, Cs; from 220 to 280°C, sharp endothermic decomposition of the anhydrous malonates gives a mixture of alkali oxalate $A_2C_2O_4$,

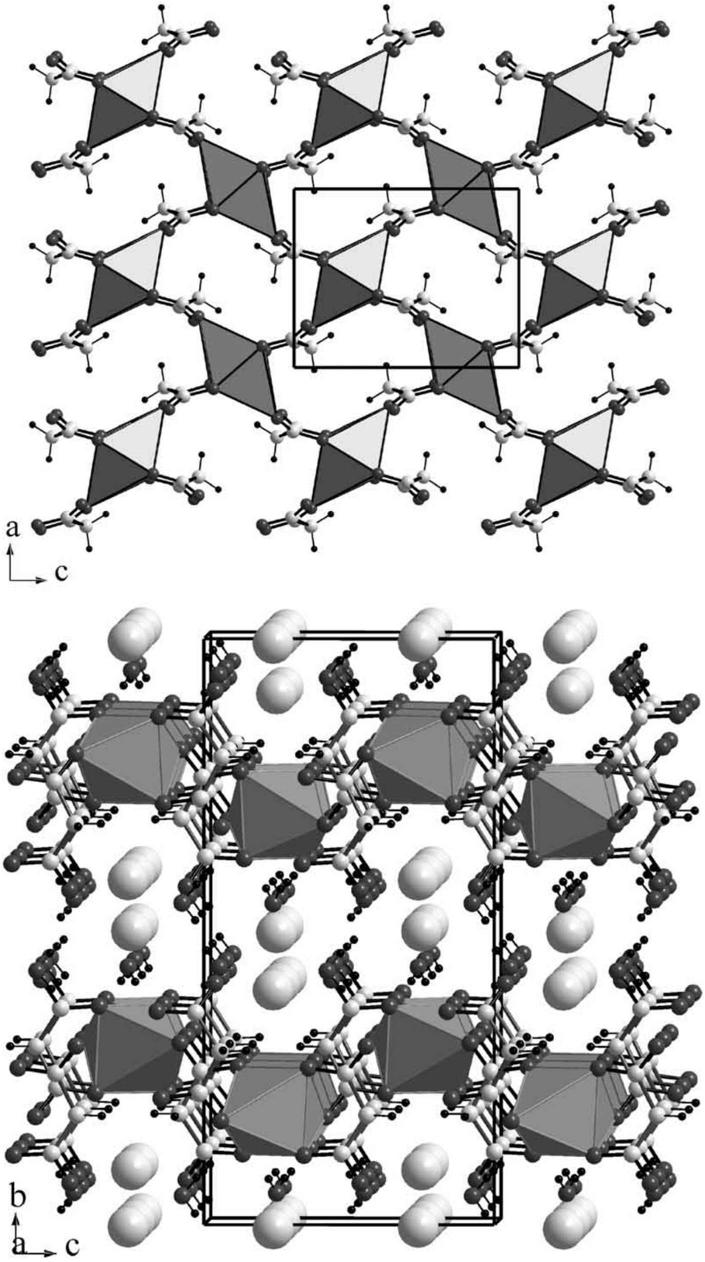

Figure 2. (Top) 2D ${}^{2}_{\infty}[\mathrm{Cu(mal)}_{4/2}]^{2-}$ anionic layer at $y = 0.25$ in **1**; (Bottom) crystal structure of **1**.

CuO and carbon accompanied by liberation of ethylene and malonic anhydride; above 360°C, weak endothermic decomposition of the alkali metal oxalate gives alkali metal carbonate A_2CO_3 with release of carbon monoxide. The thermal decomposition of the title complexes could be proposed as follows.

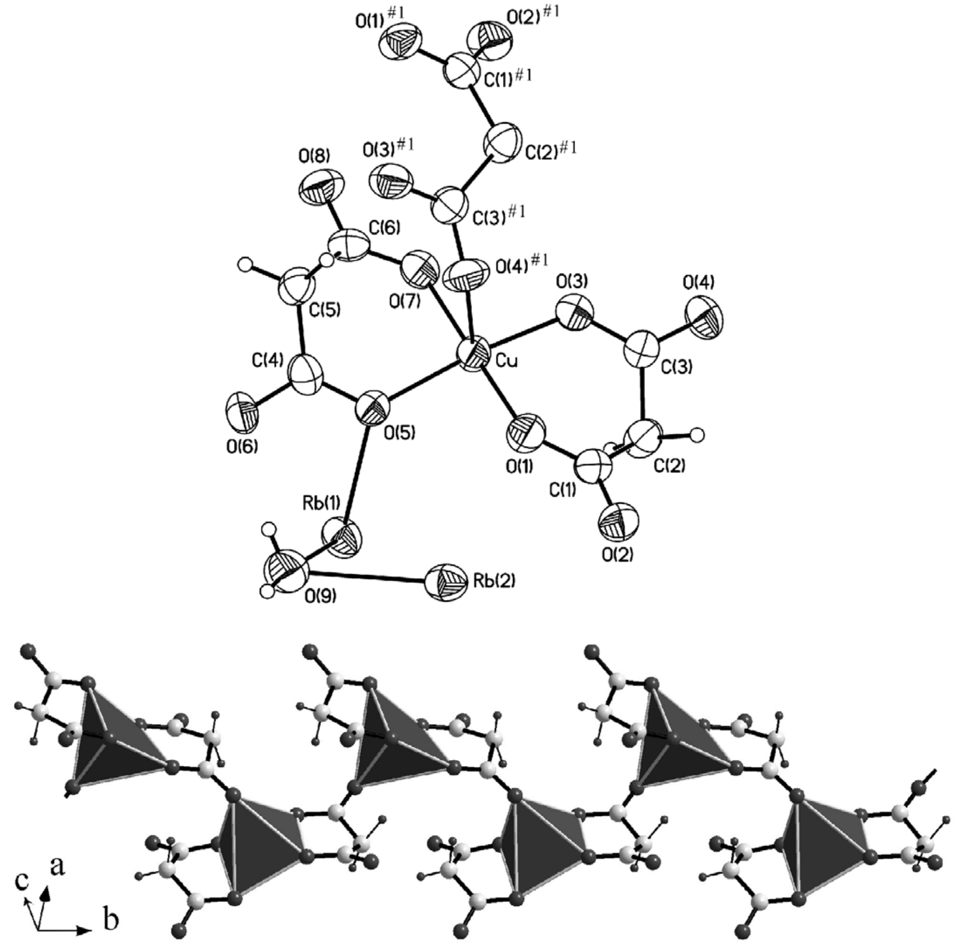

Figure 3. (Top) Ortep view of the coordination environment around Cu atoms with atom labelling for **2** (displacement ellipsoids drawn at 45% probability); (Bottom) the 1D anionic $^{1}_{\infty}[\mathrm{Cu(mal)(mal)_{2/2}}]^{2-}$ chain in **2**.

3.2. *Crystal structures*

$K_2Cu(mal)_2 \cdot 3H_2O$ (**1**) is composed of K^+ cations, lattice H_2O molecules and malonato bridged anionic layers formulated as $^{2}_{\infty}[\mathrm{Cu(mal)_{4/2}}]^{2-}$. Within the layers, Cu ions are surrounded by six oxygen atoms from four malonate anions to complete elongated octahedral coordination geometry (figure 1). Equatorial Cu–O bond distances to the chelating malonate oxygen atoms (O(1), O(3) and their symmetry equivalents $O(1)^{\#1}$ and $O(3)^{\#1}$ at $-x+1$, y, $-z+1/2$) average 1.940 Å, significantly shorter than axial bonds (2.689 Å) to non-chelating malonate oxygen atoms $O(4)^{\#2}$ and $O(4)^{\#3}$ (#2 at $-x+1/2$, $-y+1/2$, $z-1/2$; #3 at $x+1/2$, $-y+1/2$, $-z+1$). Malonate anions chelate Cu ions to form six-membered rings in a boat conformation with one non-chelating carboxylate oxygen atom at the apical position of neighboring Cu ions, resulting in 2D layers parallel to (010) as shown in figure 2. The layers are stacked along (010) so that the Cu ions of one layer are located above the apertures of the next. Lattice H_2O molecules

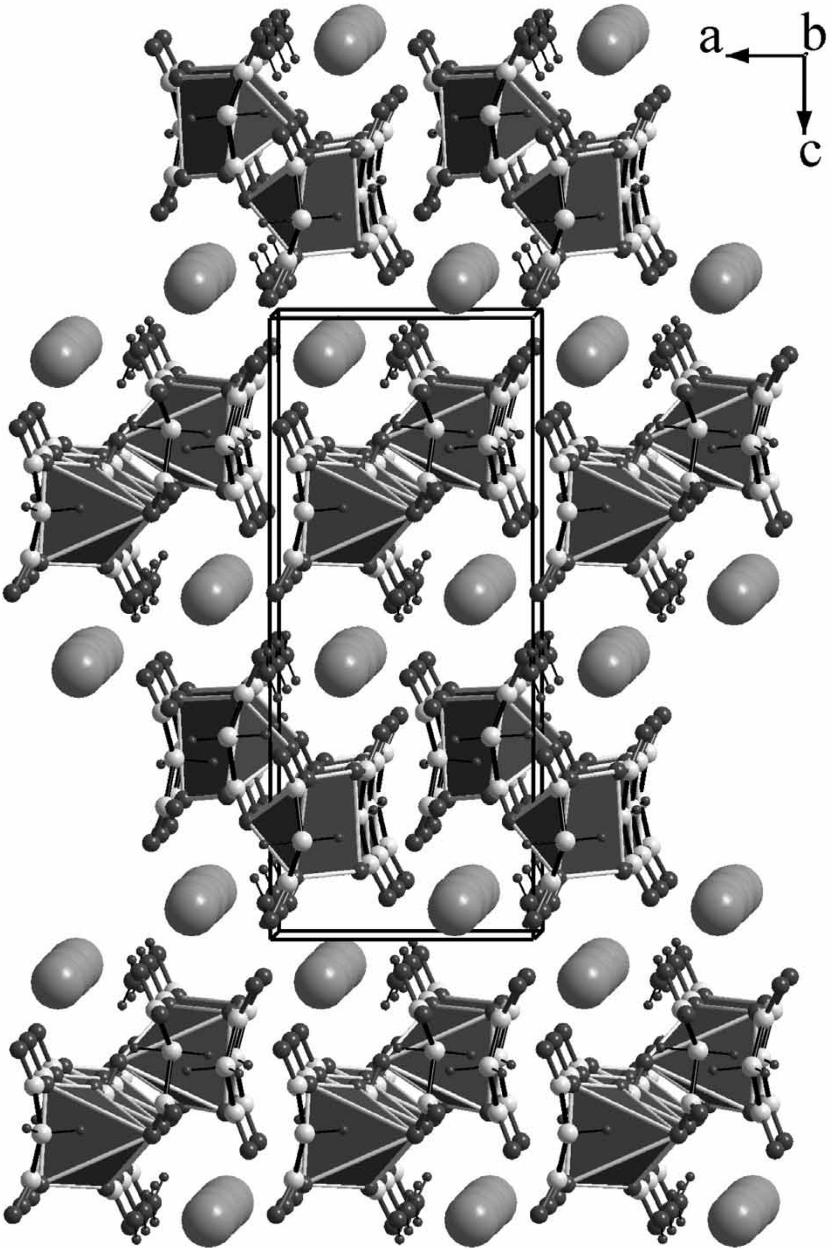

Figure 4. Crystal structure of **2**.

and K^+ cations are sandwiched between the layers (figure 2). $K^+(1)$ cations are situated at the centre of a considerably distorted pentagonal bipyramid defined by three water oxygen atoms and four carboxylate oxygen atoms with K–O contact distances in the range 2.687–2.831 Å, while $K^+(2)$ cations are surrounded by two water oxygen atoms and four carboxylate oxygen atoms at the corners of a remarkably distorted triangular

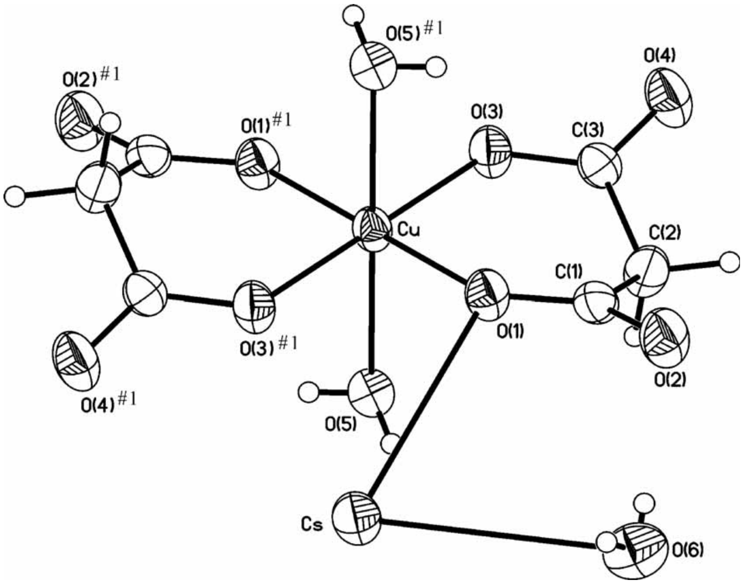

Figure 5. Ortep view of the coordination environment around Cu atoms with atom labelling for **3** (displacement ellipsoids drawn at 45% probability).

prism with K–O contact distances varying from 2.684 to 2.916 Å (table 2). Of two crystallographically distinct lattice water molecules, one (O(5)) is hydrogen bonded to two non-chelating carboxylate oxygen atoms (O(2) and O(4)) of different layers, whereas the other forms a weak hydrogen bond to the chelating carboxylate O(1) atom. The anionic layers thus are held together by lattice water molecules and the alkali cations.

The asymmetric unit of **2** contains one Cu^{2+} ion, two Rb^+ ions, one H_2O molecule and two malonate anions. In contrast to **1**, the Cu atoms in **2** are each square pyramidally coordinated by five oxygen atoms of three malonate anions with the basal plane defined by four chelating oxygen atoms (figure 3). The equatorial Cu–O bond distances fall in the region 1.917–1.930 Å and the apical Cu–O bond length is 2.597 Å (table 3). The Cu ion exhibits a slight displacement (0.069(5) Å) away from the basal plane towards the apical carboxylate oxygen $O(4)^{\#1}$ at $-x+2$, $y+1/2$, $-z+3/2$. Both crystallographically distinct malonate anions simultaneously chelate the central Cu ion through two distal carboxylate oxygen atoms to form six-membered rings with boat conformations. However, one dicarboxylate anion additionally offers one non-chelating oxygen atom to axially coordinate a Cu atom. The latter are responsible for bridging Cu atoms into anionic zigzag chains formulated as $^{1}_{\infty}[Cu(mal)(mal)_{2/2}]^{2-}$ (figure 3) that extend infinitely along (010) and are arranged according to a hexagonal packing pattern with Rb^+ ions distributed among them (figure 4). $Rb^+(1)$ is coordinated to ten oxygen atoms with Rb–O = 2.819–3.653 Å, while ($Rb^+(2)$) is bonded to nine oxygen atoms with Rb–O = 2.750–3.600 Å. Lattice H_2O molecule O(9) is bonded to both Rb^+ cations and hydrogen bonded to the non-chelating carboxylate oxygen atoms (O(6) and $O(4)^{\#7}$ at $-x+3/2$, $-y+1$, $z+1/2$). The nearly linear hydrogen bonds with $d(O\cdots O) = 2.782$, 2.853 Å (table 3) make a significant contribution to the stabilization of the lattice.

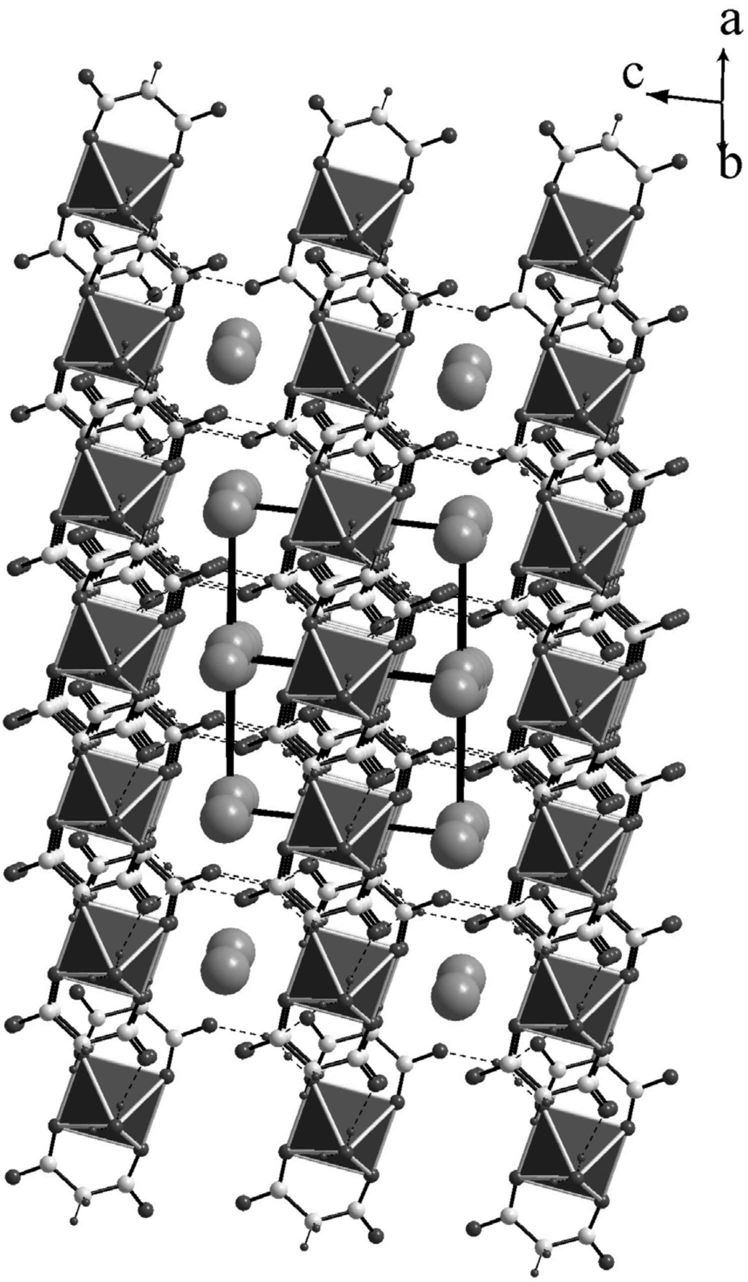

Figure 6. Crystal structure of **3**.

Compound **3** consists of Cs^+ cations, lattice H_2O molecules and $[Cu(H_2O)_2(mal)_2]^{2-}$ anions. As illustrated in figure 5, the Cu ions are each situated on an inversion centre and bonded to two *trans* aqua ligands and is chelated by two malonate anions to form six-membered rings with boat conformation. Equatorial Cu–O bond lengths are 1.936

and 1.971 Å, and the axial bond 2.418 Å (table 4). The *trans*-$[Cu(H_2O)_2(mal)_2]^{2-}$ anions are linked by interanionic hydrogen bonds between the aqua and nonchelating malonate oxygen atoms to form 1D ribbon-like chains extended infinitely in the (010) direction. The resulting anionic chains are then interconnected by lattice H_2O molecules, which are hydrogen bonded to the aqua ligand and the non-bonded carboxylate oxygen atom of the chelating malonate anions, leading to a 3D hydrogen bonded anionic framework with channels extending along the (110) direction and Cs^+ cations located within them (figure 6). The alkali cations are each surrounded by nine carboxylate oxygen atoms, two aqua oxygen atoms and two lattice water oxygen atoms with Cs–O = 3.038–4.140 Å (table 4).

In summary, the Cu ions exhibit two different coordination geometries, the "4 + 1" type in the rubidium malonate and the "4 + 2" type in the potassium and cesium malonates. The malonate anions with normal bonding values [8, 9] display two coordination modes, chelating one divalent metal atom to form a six-membered ring in boat conformation in **2** and **3** or chelating/bridging two Cu atoms in **1** and **2**. The 2D layer of Cu ions bridged by malonate anions in $K_2Cu(mal)_2 \cdot 3H_2O$ resembles that observed in $Na_2Cu(mal)_2 \cdot 2H_2O$ [18]. Substitution of the larger alkali cation results in reduction in dimensionality from 2D ${}^{2}_{\infty}[Cu(mal)_{4/2}]^{2-}$ in the potassium complex through 1D anionic ${}^{1}_{\infty}[Cu(mal)(mal)_{2/2}]^{2-}$ in the rubidium compound to *trans*-$[Cu(H_2O)_2(mal)_2]^{2-}$ anions in the cesium malonate.

Supplementary data

Crystallographic data (excluding structure factors) for the structures in this paper have been deposited with Cambridge Crystallographic Data Centre as supplementary publications CCDC 277113 ($C_6H_{10}CuK_2O_{11}$), CCDC 277114 ($C_6H_6CuO_9Rb_2$) and CCDC 277115 ($C_6H_{12}Cs_2CuO_{12}$). Copies of the data can be obtained, free of charge, on application to CCDC, 12 Union Road, Cambridge CB2 1EZ, UK (Fax: +44 1223 336033 or e-mail: deposit@ccdc.cam.ac.uk).

Acknowledgements

This project was supported by the Expert Project of Key Basic Research of the Ministry of Science and Technology of China (2003CCA00800), the Zhejiang Provincial Natural Science Foundation (Z203067) and the Ningbo Municipal Natural Science Foundation (2003A62026).

References

[1] N.L. Rosi, J. Eckert, M. Eddaoudi, D.T. Vodak, J. Kim, M. O'Keeffe, O.M. Yaghi. *Science*, **300**, 1127 (2003).

[2] M. Eddaoudi, J. Kim, N. Rosi, D. Vodak, J. Wachter, M. O'Keeffe, O.M. Yaghi. *Science*, **295**, 469 (2002).

[3] H. Li, M. Eddaoudi, M. O'Keeffe, O.M. Yaghi. *Nature*, **402**, 276 (1999).
[4] C.N.R. Rao, S. Natarajan, R. Vaidhyanathan. *Angew. Chem. Int. Ed.*, **43**, 1466 (2004).
[5] S. Kitagawa, R. Kitaura, S.-I. Noro. *Angew. Chem. Int. Ed.*, **43**, 2334 (2004).
[6] Y.-Q. Zheng, J. Sun. *J. Solid State Chem.*, **172**, 288 (2003).
[7] Y.-Q. Zheng, Z.-P. Kong. *J. Solid State Chem.*, **166**, 279 (2002).
[8] C. Ruiz-Pérez, M. Hernández-Molina, P. Lorenzo-Luis, F. Lloret, J. Cano, M. Julve. *Inorg. Chem.*, **39**, 3845 (2000).
[9] S. Konar, P.S. Mukherjee, M.G.B. Drew, J. Ribas, N.R. Chaudhuri. *Inorg. Chem.*, **42**, 2545 (2004).
[10] Y.-Q. Zheng, J.-L. Lin, Z.-P. Kong. *Inorg. Chem.*, **43**, 2590 (2004).
[11] Y.-Q. Zheng, H.-Z. Xie. *J. Coord. Chem.*, **57**, 1537 (2004).
[12] R.L. Carlin. *Magnetochemistry*, Spinger-Verlag, Berlin (1986).
[13] G.M. Sheldrick. *SHELXS-97, Programm zur Lösung von Kristallstrukturen*, University of Göttingen, Germany (1997).
[14] G.M. Sheldrick. *SHELXL-97, Programm zur Verfeinerung von Kristallstrukturen*, University of Göttingen, Germany (1997).
[15] E.-B. Ying, Y.-Q. Zheng, H.-J. Zhang. *J. Mol. Struct.*, **693**, 73 (2004).
[16] Y.-Q. Zheng, E.-B. Ying. *Z. Kristallogr. NCS*, **219**, 423 (2004).
[17] K. Nakamoto. *Infrared Spectra of Inorganic and Coordination Compounds*, Wiley-Interscience, New York (1970).
[18] J.C. Barnes, T.J.R. Weakley. *Acta Crystallogr.*, **C53**, 26 (1997).